International Journal of Engineering Trends and Technology
ISSN: 2231-5381/ https://doi.org/10.14445/22315381/IJETT-V74I8P117
Volume 74 Issue 8, 249-258, August 2026

Original Article

Study of Tie Down Clamping System for Port Crane

Yeon Taek OH

Department of Mechanical Engineering, Tongmyung University, 428 Sinseon-ro, Nam-gu, Busan, South Korea.

Corresponding Author: yeonoh@tu.ac.kr

Received: 20 February 2026 Revised: 16 June 2026 Accepted: 15 July 2026 Published: 29 August 2026

Abstract - *This study examines a port crane securing system. A securing system, often referred to as a tip-over prevention device, prevents cranes from overturning caused by strong winds or typhoons, and this tie-down system is attached to each leg of a crane and designed to withstand wind speeds of up to 50 m/s. Conventional crane securing systems are frequently identified as challenging and time-consuming to install. However, this study proposes a securing system applied with an automated tie-down system that overcomes these shortcomings. The proposed securing system that utilizes an automated tie-down mechanism is designed to replace the manual tie-down method with a self-fastening mechanism to prevent the crane from overturning, capsizing, and slipping due to typhoons and strong winds and to ensure structural safety. A combination of geared motors and springs were used in the upper and lower securing points to achieve automatic fastening. Furthermore, this study was able to ensure the stability and reliability of the securing system by verifying the proposed system's structural integrity through structural and dynamic analyses using software.*

Keywords - *Tie down clamping system, Stress analysis, Locking structure, Multi-Body Dynamics analysis, Tie down alignment, Port crane, Stowage pin.*

1. Introduction

As port congestion has emerged as one of the major causes of the unprecedented crisis in global supply chains brought by the COVID-19 pandemic that swept through the world, the need for automated ports has drawn significant attention. Moreover, the world is undergoing rapid shifts driven by an accelerating pace of technological advancements, known as the Fourth Industrial Revolution, and the global port industry is experiencing a significant transformation. Based on the rapid innovation and convergence of information and communication technologies, technological advancements in the port industry are heavily focused on accelerating operational efficiency through the development of unmanned and automated ports.

The development and advancement of next-generation container terminals for unmanned automation prioritizes three core pillars: safety, productivity, and environment. These must be secured to enhance port competitiveness, and port automation is regarded as a necessity rather than a mere option. Port automation is improving port productivity and efficiency while preventing safety accidents by introducing unmanned container transport equipment, specifically Automated Guided Vehicles (AGVs), and operating automated systems. The development of unmanned cranes has enhanced efficiency, with data confirming that automation can increase operational speed by up to 30%, depending on the skills of crane operators.

Furthermore, the components of port logistics automation can be broadly categorized into four systems. First, Container Vessel & Container involve the automated loading and unloading of containers from ships. Second, the AGV system is an unmanned automatic system that transports loaded or unloaded containers from ships within the yard. Third, the Rail Mounted Gantry Crane (RMGC) & Yard is a specialized, fully automated, and unmanned system that manages the stacking and retrieval of containers transported by AGVs. Fourth, the Gate and Railway system moves containers into and out of a container yard.

Port logistics automation is a system that can organically integrate and control the above-described four systems, and the development and configuration of optimal System Integration (SI) is considered the core of port automation.

Even with advanced, automated port logistics systems, swift and safe crane securing with anchoring devices often still relies on manual intervention during sudden gusts, high winds, or typhoons. For this reason, the need for the development of an automated securing system that can counteract malfunctions. Crane securing is achieved using stowage pins and tie-downs. Stowage pins are used to prevent cranes from moving, while tie-downs prevent them from overturning. Thus, stowage pins prevent horizontal movement of the crane, while tie-downs are used to counteract vertical uplift forces acting on cranes.

Fig. 1 Stowage and tie down

Fig. 2 Example of the installation of a storage on a port and crane

A stowage pin, often referred to as a crane anti-slip device, is designed to secure cranes from being moved or pushed by high winds when they are not in operation and moored in the stowage position.

Two sets of rail clamps, one for the land side and one for the sea side, are installed on a support at the center of the sill beam. Operating two sets of rail clamps involves stopping the crane at the designated mooring location, then releasing the safety pin on the manual operation lever connected to the pin. The operational sequence is followed by raising the lever, which forces the stopping pin down into the mooring anchor socket. After removing the anchor fixing pins and installing the anchor, the operating lever must be secured in a position that prevents it from dropping down due to its own weight.

A proximity limit switch is installed to monitor for any loosening of the anchor and to interlock the anchor with the driving device. The proper operational procedure is as follows: First, the stop pin must be released before starting work, and the anchor must be returned to its original position to prevent it from falling during operation. Lastly, the stop pin must be used to moor the crane when the operator stops work or leaves the crane unattended.

Tie-downs (anti-tip devices) are designed as tip-over prevention devices that prevent cranes from overturning during high winds or typhoons. They are attached to each leg of a crane and designed to withstand wind speeds of up to 50 m/s.

The tie-down system securing the crane leg to the base metal (crank) embedded in the port's driveway floor is connected by a chain and turnbuckle assembly fixed to the crane leg. Tie-downs are tightened to support the loads during crane mooring. While the crane is in operation, connecting bolts to the base metal (crank) are removed by loosening the turnbuckle, and the crane shaft is secured.

Fig. 3 Example of the installation of a tie down on a port and crane

This research focuses on an automated tie-down system that can automatically secure cranes by replacing the manual tie-down method to prevent them from overturning, capsizing, and sliding during extreme wind events such as typhoons and to ensure structural safety.

2. Structure of Tie Down

The upper tie-down unit consists of a linear bushing, TM screw, spur gear module, geared motor, hydraulic cylinder, and guide roller. As shown in the Figure 5, the geared motor drives a spur gear, which in turn drives a gear fixed to a TM Bolt. This bolt is rotated to create vertical movement of the lower module of the upper tie-down system. The four linear shafts attached to the upper tie-down unit act as a structural guidance system to ensure the lower module moves up and down without unwanted rotational movement.

The crank of the lower tie-down unit is anchored to the ground, and the alignment of the lower module of the upper securing device is positioned using linear rollers. Once the alignment is verified, the lower module and the crank are securely connected using a hydraulic cylinder.

Figures 4 and 5 illustrate the overall and detailed structures of the tie-down system. Table 1 presents the specifications of the tie-down system developed in this study.

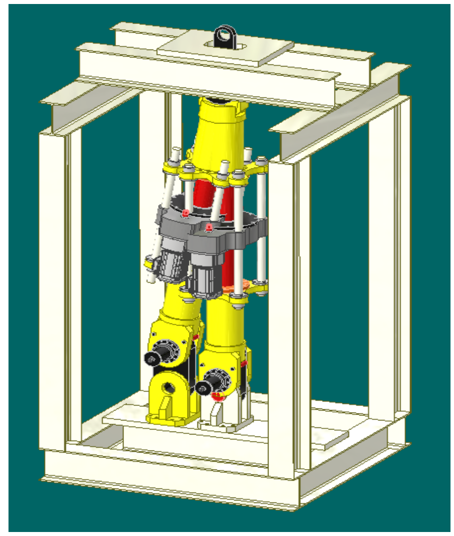

Fig. 4 Tightness of a tie-down system

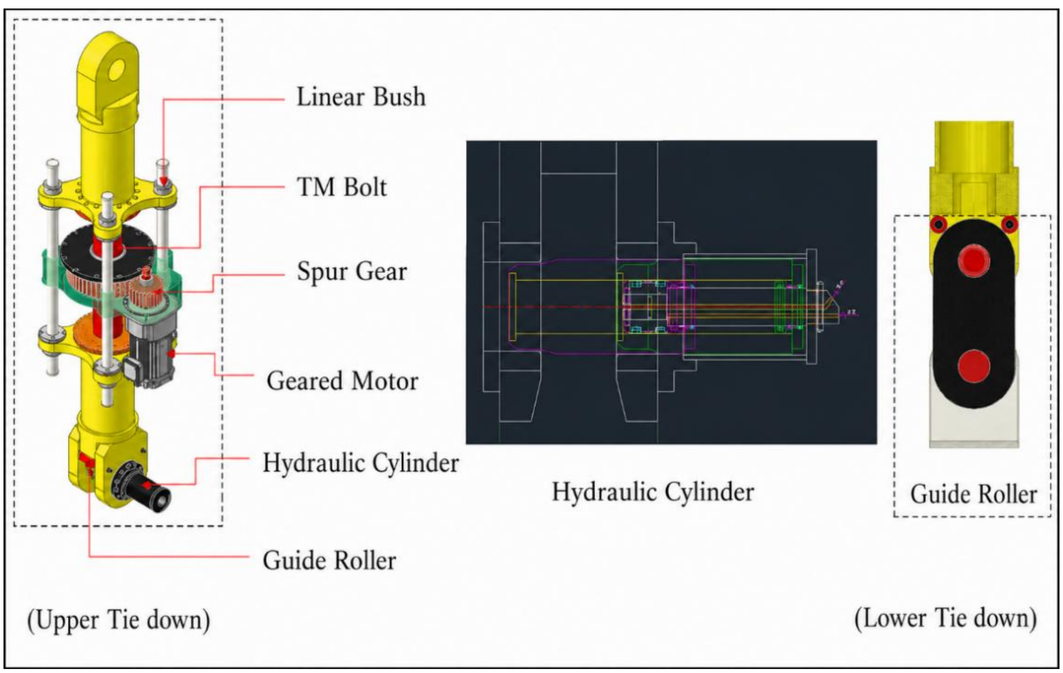

Fig. 5 Tightness of a tie-down

Table 1. Specification of tie down system

Parts	Value
Size (L*W*H mm)	2,000 x 2,000 x 4,000
Weight	MAX. 5.0ton
Speed	80mm/sec
Stroke	700mm
Power	2.2kw
Angle	±7˚

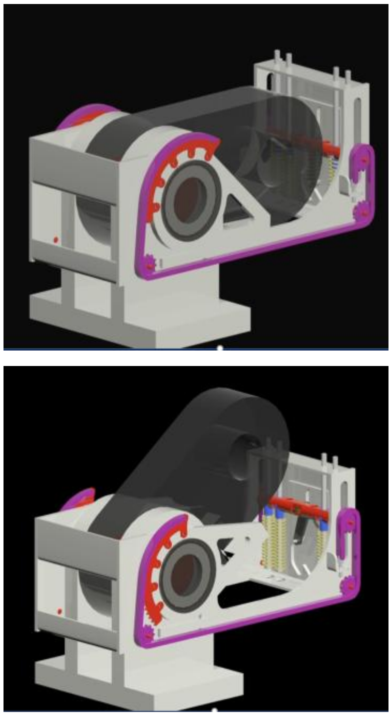

Fig. 6 Lower tie down & crank

Figure 6 shows the structure of the lower tie-down device installed on the port ground. The crank of the lower securing device is designed to rotate 90 degrees from a horizontal to a vertical position using spring force.

The crank can be tilted with a minimal force of approximately 7 kg by incorporating a mechanical, non-powered shock absorber. As shown in Figure 7, when the fixing device is released by four springs arranged in parallel, the spring force transmitted to a chain is converted into rotational force by a sprocket fixed to the crank, and the resulting torque rotates the crank. Figure 7 represents the principle of movement involving four springs to alternate between compression and tension.

Figure 8 shows a locking structure that secures a spring. A pin connected to a shaft fixed with a spring is designed to move along a groove. The pin is attached to a spring shaft with one end of a spring fixed. For this reason, when the spring is compressed or extended, the pin locks into place at the designed maximum or minimum stroke. Thus, the pin is structured to lock as it moves along a groove. When the pin is pressed while the spiral link is engaged, the locking mechanism is released and spring forces the lower link to rise.

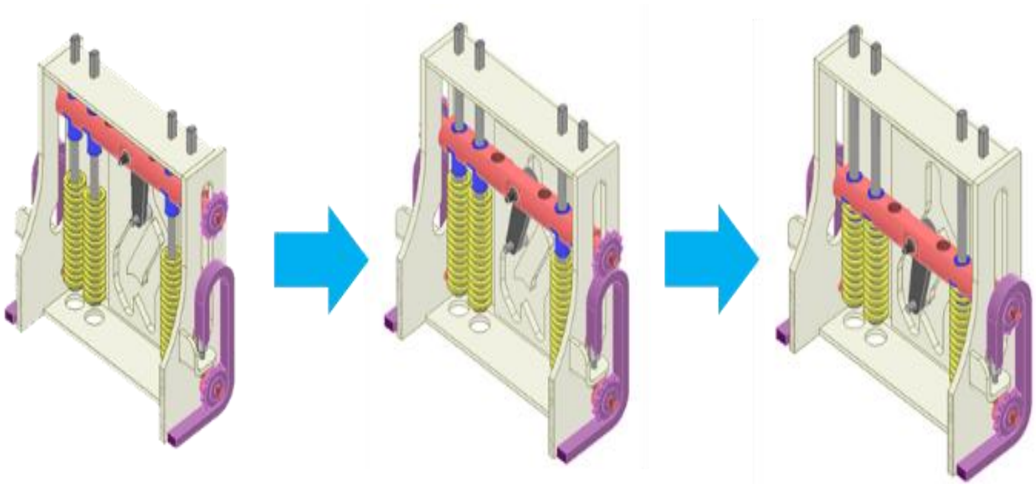

Fig. 7 Principle of spring operation

Fig. 8 Locking structure of lower tie-down

Table 2. Specification of spring

Parts	Free Length	Initial Setting Length	Max. Comp. Length
SSL 35x200 (1.08 kg/mm)	200mm	195mm	95mm
SSL 40x250 (1.73 kg/mm)	250mm	230mm	130mm
Etc.	Spring Stroke: 100mm		

Two types of springs were used in the lower tie-down unit. The spring constants of the two types are 1.08 kg/mm and 1.73 kg/mm, as shown in Table 2. The change in spring length during the lower tie-down movement is presented in the above Table. In the fastening process of the tie-down system, when a spring force causes the crank to rotate from a horizontal to vertical position, the lower module of the upper tie-down moves downwards by the geared motor. When the lower module of the upper tie-down and the crank are aligned by the guide roller, they are fastened together with pins by the hydraulic cylinder.

3. Structural Analysis of Tie Down

Figure 9 represents the structure of the upper tie-down attached to the crane body. The upper tie-down system is mainly composed of three modules: an upper module including the TM Nut (R) at the top; a lower module including the TM Nut (L) at the bottom; and a central module including the TM Screw, a motor that provides the rotational force to the screw, and a guide that ensures the upper and lower modules to move in a linear path. The top module is connected directly to the crane's body, and the upper and lower modules are secured by the TM Screw of the central module and together with nuts of the upper and lower units. The lower module and the crank of the lower tie-down unit are connected using a pin to anchor the crane.

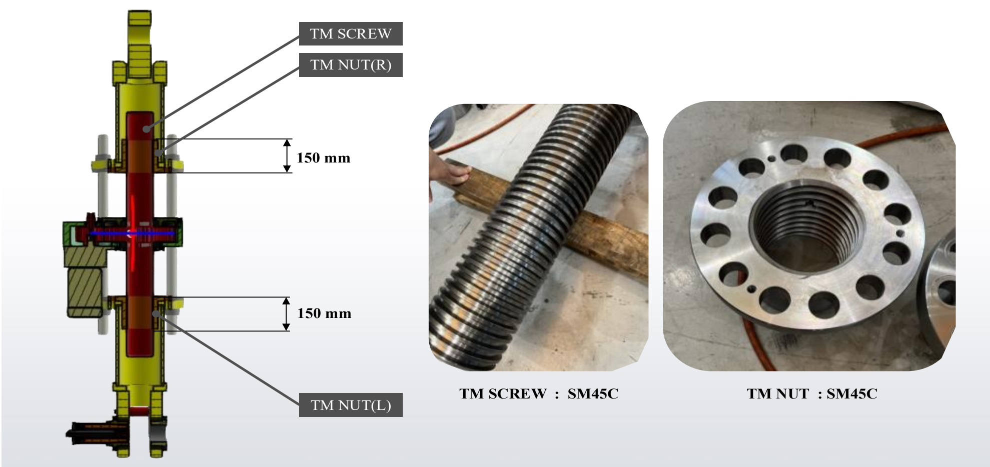

Fig. 9 Structure of upper tie down

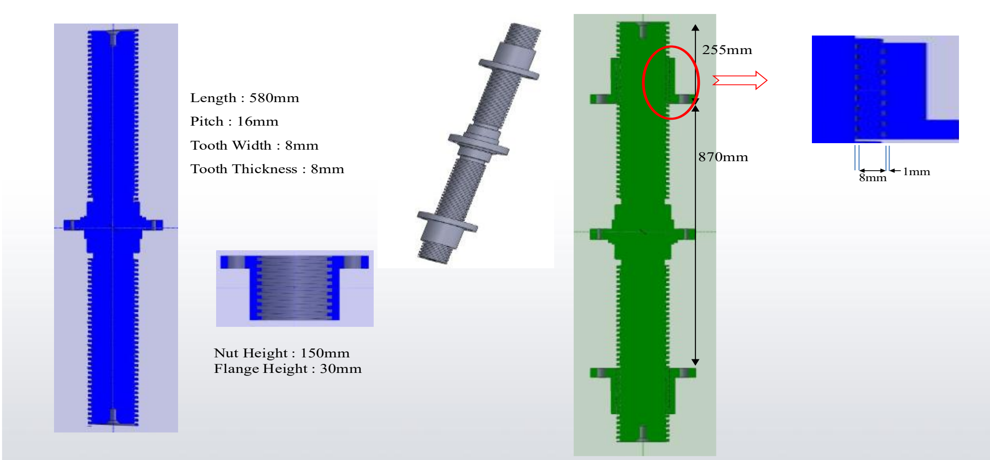

Fig. 10 Structure TM Screw & TM Nut

First, the structural analysis of TM Screw and TM Nut was conducted by applying a load to TM Screw and TM Nut connecting the central module of the upper tie-down and upper/lower modules when the upper and lower tie-down units are connected. The TM Screw has a square-shaped structure with a pitch of 16 mm, a tooth width of 8 mm, and a tooth thickness of 8 mm. In addition, the TM Nut is designed to have a helical structure of 150 mm length that matches the TM Screw that interlocks with the length of the nut when fastening the securing system. The structural analysis was performed based on the assumption that the TM Screw and TM Nut exhibit integral behavior while maintaining sliding contact within structural analysis.

The boundary condition was analyzed by assuming that the bottom surface of the nut flange of the lower module is constrained, and a 300-ton load is applied to the flange of the upper module in the upper tie-down. The 300-ton load is a maximum allowable load placed on a single tie-down of a crane when a wind speed of 50 m/s occurs during a typhoon.

The analysis results showed that the maximum Von Mises stress was 1205.41 N/mm^2 in integral contact. Approximately 0.9% of the total area exhibited a von Mises stress distribution of 1104-1205 N/mm^2.In sliding contact, the maximum Von Mises stress was 1580.84 N/mm^2, higher than in bonded contact. The Von Mises stress distribution ranged from 1580.84 to 1449.11 N/mm^2 in approximately 1.2% of the total area.

The higher Von Mises stress observed in sliding contact compared to bonded contact is because the vertical direction is fixed at the boundary surface, while sliding occurs in the horizontal direction. The Von Mises stress was higher in sliding contact compared to bonded contact.

Thus, the stress is higher in a contact surface where is fixed in only one direction compared to two directions. Figure 11 shows the shear surface where the maximum Von Mises stress occurs, and the maximum stress occurs at a similar location to the shear surface.

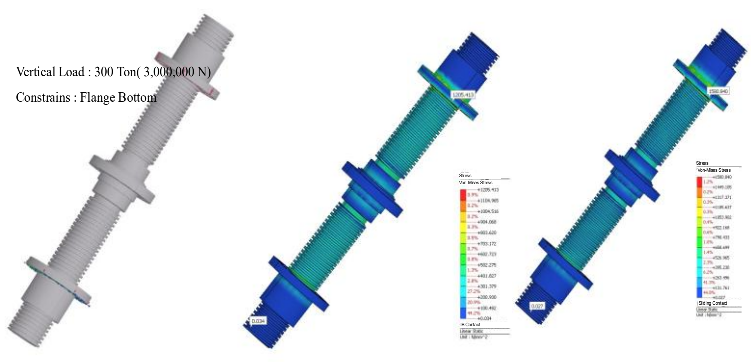

(Boundary Condition) (Stress_Integrated Behavior Contact) (Stress_Sliding Contact)

Fig. 11 Boundary condition, structure analysis & Von Mises stress

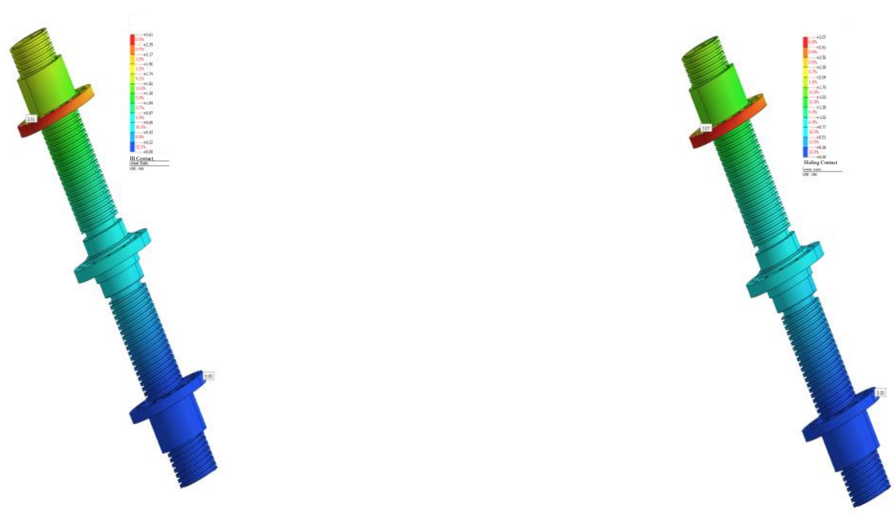

(Strain_Integrated Behavior Contact) **(Strain_Sliding Contact)**

Fig. 12 Max strain position

Figure 12 presents the maximum strain of the TM Screw after structural analysis under the same boundary condition in the above. Figure 12 shows the analysis results of maximum strain of the TM Screw after structural analysis.

The maximum displacement was 2.61 mm in bonded motion, and the displacement occurring in the direction of the TM Screw's axis was 3.07 mm. The analysis results suggest that stress levels and displacements are within safe limits based on a review of the material properties and the securing system.

After analyzing the upper tie-down system, a structural analysis of the lower tie-down system was conducted. Figure 13 shows the structure of the lower tie-down. A spring installed inside the right side of the lower tie-down unit is designed to lift up a crank on the left side connected by a chain to a spring-loaded shaft.

Four springs are arranged in parallel, and the chain connected to the sprocket at the end of the springs rotates. The figure below shows the specifications of the spring used. The initial conditions of springs within the lower tie-down unit are described in Table 2.

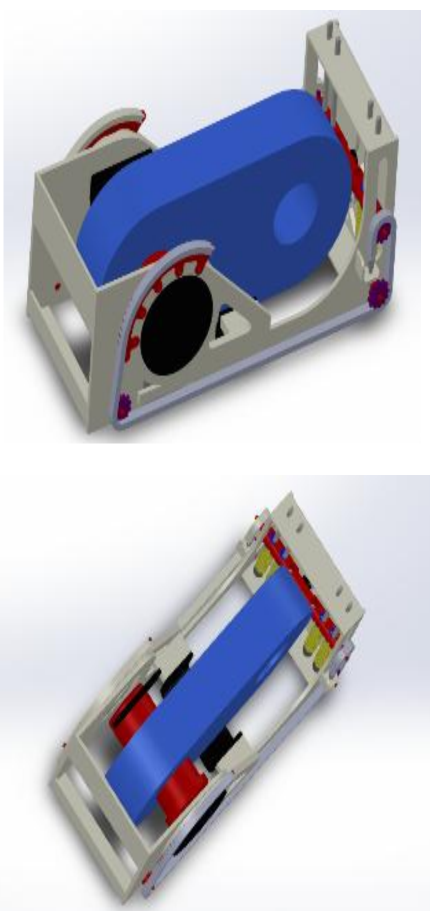

Fig. 13 Structure of lower tie down

Model	Outer Dia (mm)	Inner Dia (mm)	Free Length (mm)	Spring Constance (kgf/mm)
35×200	35	21	200	1.08
40×250	40	26	250	1.73

Model	0.3mm		0.5mm		1mm	
	Deflection (mm)	Load (kgf)	Deflection (mm)	Load (kgf)	Deflection (mm)	Load (kgf)
35×200	100	108	90	97	80	86
40×250	100	173	90	156	80	138

Fig. 14 Specification of spring

For the dynamic analysis, a modeling was employed based on the design drawings of the lower tie-down's sprocket and crank assembly, incorporating detailed spring specifications. Since the simulation software lacked specialized modules for a coupled analysis of a sprocket and chain linkage system, the system was divided into crank and spring sections and analyzed separately. In sprocket modelling, the assembly was configured by arranging a revolute joint between the crank and the body, while fixing the body as a constrain. In the revolute joint, the crank was set to rotate 90° for two seconds to produce a vertical lifting motion. Figure 15 represents the results of the driving process in the simulation program. The simulation results revealed that an initial driving torque of 217,937 N·mm was required at the start of a lift of the crank. Thus, the driving torque is generated by a force transmitted to a chain from a spring on the opposite side. The distance between the center of the crank and the sprocket pitch circle was 137.5mm. Therefore, the minimum force required to lift a crank system was determined to be 1585N.

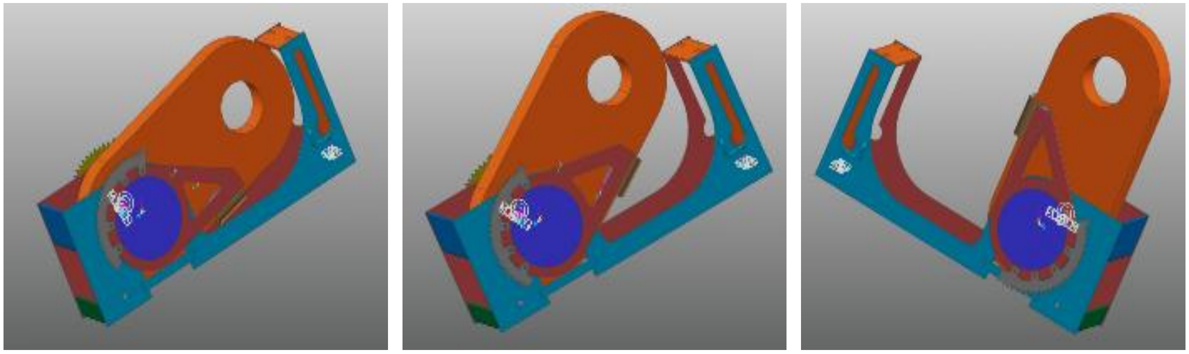

Fig. 15 Simulation result of crank modelling

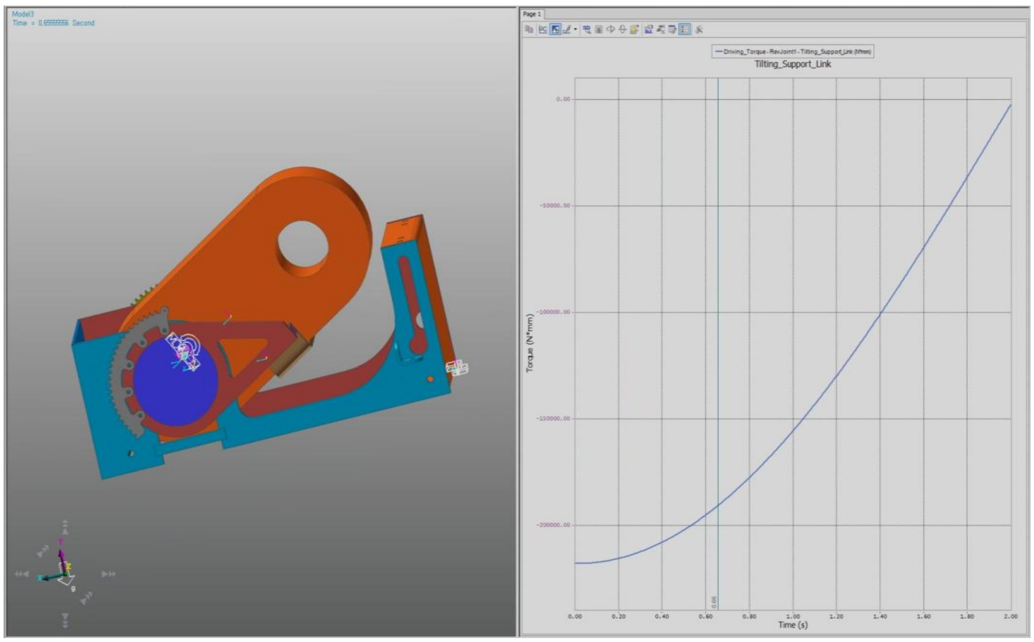

Fig. 16 Driving torque of bracket lift up

Figure 16 shows that the driving torque varies with the change in crank angle in dynamic analysis. The driving torque reached its maximum value when the crank started to rotate.

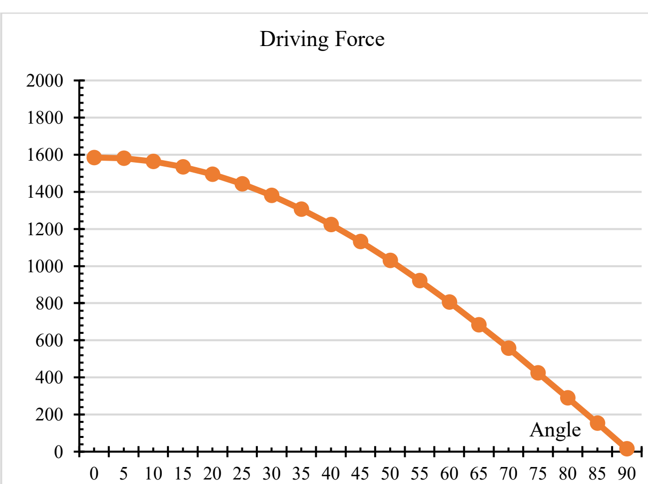

Fig. 17 Force of Bracket Lift Up

Figure 17 shows the result of the conversion of torque into force in dynamic analysis. The required initial drive torque was 1580 N to lift up the crank, and the force gradually decreased as the lift progressed. Therefore, the upward force exerted by the spring in the lower tie-down must exceed the driving force for the system to lift the crank.

Figure 18 illustrates the spring modelling of the lower tie-down system. Four springs consisting two types of springs are installed on the side of the lower tie-down. Four springs attached to the shaft horizontally on the side, and four columns with inserted springs serve as the guiding mechanism for vertical movement.

A spring is initially compressed and secured to a shaft by a rotating pin. When a pin connected to a fixed shaft is released, a compressed spring expands to generate spring force. This spring force is transmitted to a chain connected to the end of the shaft and lifts up a crank located on the opposite end.

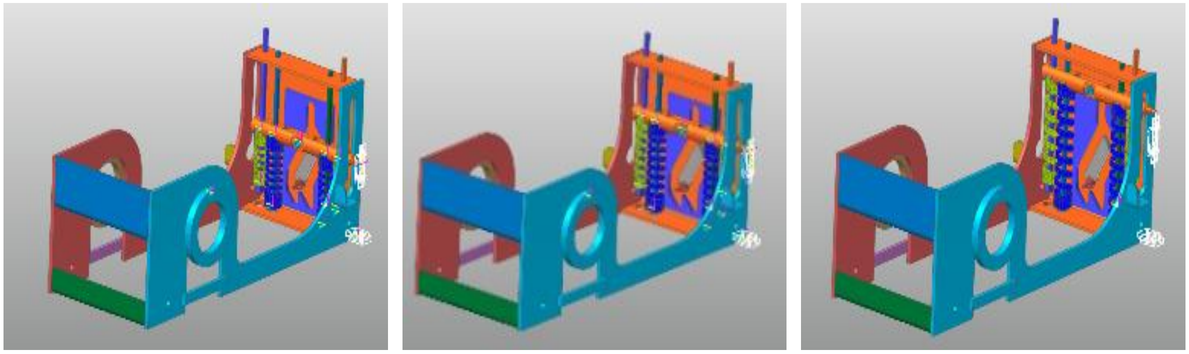

Fig. 18 Simulation result of spring modelling

Figure 19 shows the results of the spring module simulation. The spring force was 6746 N at initial tension in a spring at the moment a pin was released from a compressed state, and the final spring force was 1233 N at a displacement of 100mm. Figure 19 presents the spring force generated when the spring was tensioned as a result of the simulation.

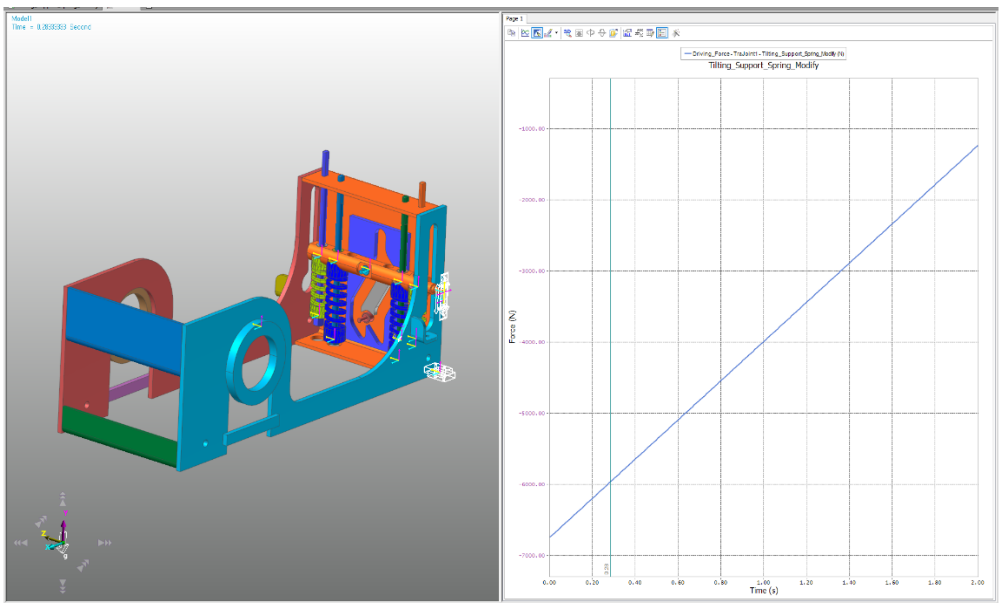

Fig. 19 Result of spring model simulation

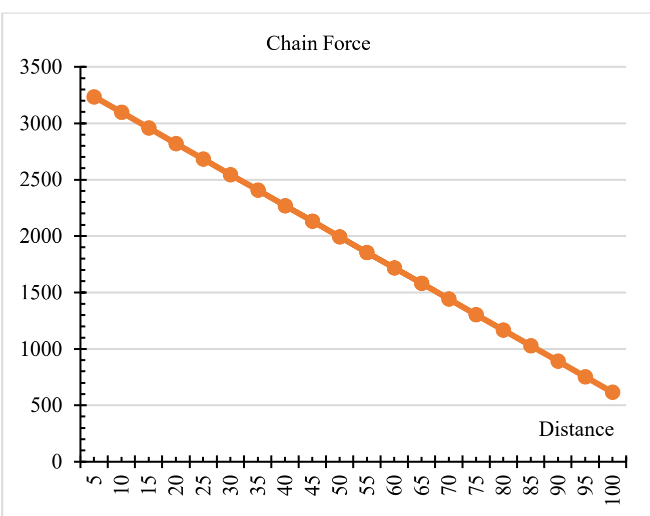

Fig. 20 Chain Force

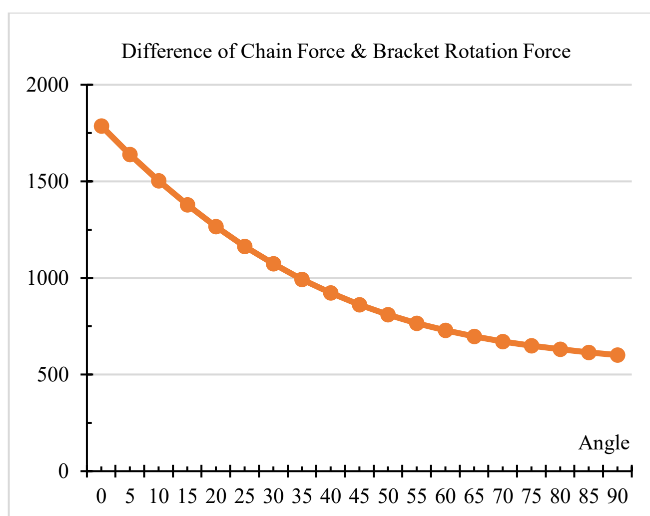

Fig. 21 Difference of chain force & bracket rotation force

Figure 20 shows the force transmitted by the spring force to the chain. The force transmitted to the chain is only half of the spring force because a small sprocket connected to a chain and shaft has a similar structure to a pulley. The comparison of crank rotational force and the force acting on a chain demonstrates that the force acting on a chain is high enough to lift a crank.

4. Conclusion

The securing system installed on port cranes serves a crucial role in preventing cranes from collapsing during typhoons and extreme wind gusts. However, this tie-down system is often manually operated, requiring worker intervention to secure a device. Each crane is typically supported by four to six columns, and tie-downs are installed on both the landside and seaside. Securing a crane often requires 8 to 12 lashing units per crane. Moreover, lower lashing device cranks require a forklift or other equipment to lift, which adds complexity. Securing lashing units for a single crane requires significant labour-intensive and time-consuming efforts. Therefore, this study proposes a securing system that utilizes a spring-based lower tie-down system that allows workers to easily secure cranes without any assistance, such as a forklift. Furthermore, to verify the structure of the proposed system, structural and dynamic analyses were performed using software to ensure the stability and reliability of the securing system.

Acknowledgments

This Research was supported by the Tongmyong University Research Grants 2023. (2023A020)

References

[1] Brian McDonald, Bernard Ross, and Robert A. Carnahan, “The Bellevue Crane Disaster,” *Engineering Failure Analysis*, vol. 18, no. 7, pp. 1621-1636, 2011. [CrossRef] [Google Scholar] [Publisher Link]

[2] Jae-Hwan Lee et al., “Wind Force Coefficients Computation of Gantry Crane by Wind Tunnel Experiment and Structural Analysis of the Crane,” *Journal of the Society of Naval Architects of Korea*, vol. 48, no. 2, pp. 165- 170, 2011. [CrossRef] [Google Scholar] [Publisher Link]

[3] Lee Seong Wook et al., “The Effect of Wind Load on the Stability of a Container Crane,” *Journal of the Korean Society of Precision Engineering*, vol. 22, no. 2, pp. 148-155, 2005. [Google Scholar]

[4] Dong-Hyawn Kim, Byung-Cheol Oh, and In-Sik Chun, “Effect of Wind Velocity Variation on Safety Factor of Container Crane Tie-downs,” *KSCE Journal of Civil and Environmental Engineering Research*, vol. 25, no. 6A, pp. 1127-1131, 2005. [Google Scholar] [Publisher Link]

[5] Dong-Seop Han, and Geun-Jo Han, “Force Coefficient at each Support Point of a Container Crane According to the Wind Direction,” *International Journal of Precision Engineering and Manufacturing*, vol. 12, no. 6, pp. 1059-1064, 2011. [CrossRef] [Google Scholar] [Publisher Link]

[6] Dong-Seop Han, and Geun-Jo Han, “The Difference in the Uplift Force at each Support Point of a Container Crane between FSI Analysis and a Wind Tunnel Test,” *Journal of Mechanical Science and Technology*, vol. 25, no. 2, pp. 301-308, 2011. [CrossRef] [Google Scholar] [Publisher Link]

[7] Chan K. Yang, and M.H. Kim, “The Structural Safety Assessment of a Tie-Down System on a Tension Leg Platform During Hurricane Events,” *Ocean Systems Engineering*, vol. 1, no. 4, pp. 263-283, 2011. [CrossRef] [Google Scholar] [Publisher Link]

[8] Rong Gao et al., “The Simulation of Rotary Motion of the Flexible Multi-Body Dynamics of Tower Crane,” *Advanced Materials Research*, vol. 655-657, pp. 281-286, 2013. [CrossRef] [Google Scholar] [Publisher Link]

[9] Juhwan Choi, and Jin Hwan Choi, “Analysis Method for Multi-Flexible-Body Dynamics Solver in RecurDyn,” *The Korean Society of Mechanical Engineers*, vol. 3, no. 2, pp. 107-115, 2015. [Google Scholar] [Publisher Link]

[10] Guang Yang, Lan Yang, and Meng Cao, “Simulation Analysis of Timing Belt Movement Characteristics based on RecurDyn,” *Vibroengineering Procedia*, vol. 22, pp. 13-18, 2015. [CrossRef] [Google Scholar] [Publisher Link]

[11] Wisnu Wardhana, Yoyok Setyo Hadiwidodo, and Faisal Siswanto, “Strength Analysis and Sea-Fastening Design of Container Crane Structure for Heavy Lifting Sea Transportation,” *Applied Mechanics and Materials*, vol. 874, pp. 147-154, 2015. [CrossRef] [Google Scholar] [Publisher Link]